Macromolecules

pubs.acs.org/Macromolecules Article

High-Strength Polyurethane Elastomer with Phototunable Mechanical Properties and Fluorescence

Zixin Li, Xinyu Li, Zhiqi Zhang, Jing Bai,* and Fei Chen*

Cite This: *Macromolecules* 2025, 58, 9799−9808 Read Online

ACCESS | Metrics & More | Article Recommendations | Supporting Information

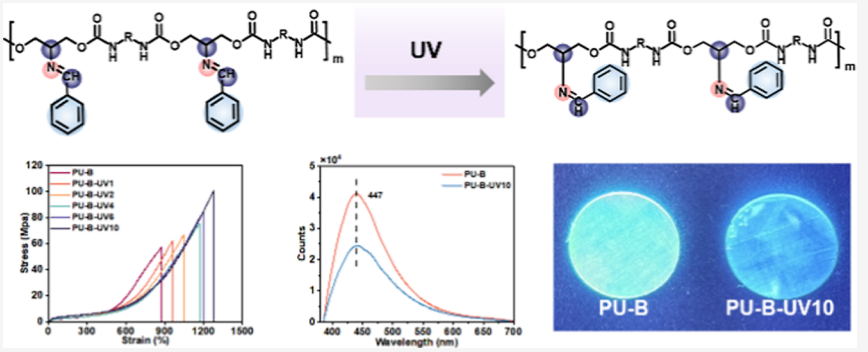

ABSTRACT: A high-performance polyurethane elastomer with conjugated structures on chains was designed and synthesized. First, the $\pi-\pi$ conjugated interaction can enhance the mechanical properties of polyurethane via noncovalent cross-linking without ruining recyclability. Meanwhile, due to the photocontrolled cis−trans isomerization of imine bonds, the conjugation of the aromatic rings exhibited a UV light-controllable characteristic, thereby enabling the control of the mechanical properties of polyurethane with UV light. The fluorescence properties of the conjugated structure can also be controlled by UV light via photoisomerization of C═N. Therefore, in this study, a kind of polyurethane elastomer with UV light-controllable mechanical properties and fluorescence emission was obtained. While its mechanical performance is tuned by UV light, it can also be applied in the area of information storage due to its tunable fluorescence. Patterns and information can be written on the polyurethane film via UV light irradiation.

INTRODUCTION

Polyurethane is widely used in multiple fields in people's daily lives due to its excellent performance and the strong designability of its structure and performance. With the development of science and technology, further requirements have been put forward for the performance of the materials. For polyurethanes, it is required that they possess excellent performance while also having the characteristic of recyclability and reprocessability.[1−3] Therefore, the traditional strategy of enhancing the performance through cross-linking is no longer applicable. Currently, in these areas, the construction of polyurethane with the participation of dynamic bonds is mostly used to achieve the balance between performance enhancement and recyclability.

$\pi-\pi$ conjugation is a noncovalent interaction that exists between aromatic structures containing π orbitals. The $\pi-\pi$ conjugation effect arises from the attractive interaction between electron clouds with different charges within the aromatic systems.[4−6] This interaction can be classified into two types: (i) face-to-face stacking and (ii) edge−face stacking. Their energy levels are approximately 1 to 50 kJ·mol^{-1} for the stacking of benzene rings, with most falling around 10 kJ·mol^{-1} or lower.[7] The $\pi-\pi$ conjugation, as a topical noncovalent dynamic bond, has also received extensive attention from researchers, and some works have achieved encouraging results. Lu's group[8] designed and synthesized a series of PU with a biphenyl structure on the chains. The $\pi-\pi$ conjugation and cation−π interactions of biphenyl enhanced the strength and toughness of the material. Du[9] designed an elastomer with a novel chain extender featuring a phenylurea group at the end with dense hydrogen bonds and $\pi-\pi$ interactions, which imparts strong mechanical properties. Zhou and Song[10] prepared a series of high-strength flame-retardant polyurethanes using a chain extender with phosphorus-containing conjugated groups. Due to the $\pi-\pi$ stacking effect, the mechanical strength of this kind of polyurethane was significantly enhanced. The breaking strength was 57 MPa, and the elongation at break was 2260%. The toughness was 460 MJ/m^3, and the true fracture stress was as high as 1.34

Received: July 2, 2025
Revised: August 27, 2025
Accepted: August 29, 2025
Published: September 3, 2025

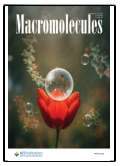

https://doi.org/10.1021/acs.macromol.5c01778
Macromolecules 2025, 58, 9799−9808

GPa, which exceeded the true fracture stress value of all of the previously prepared polyurethane elastomers. This kind of polyurethane film can even lift an object that is 100,000 times heavier than itself. Further, Dong's group[11] designed a polyurethane system with both aromatic and temperature-responsive dynamic bonds. The strong $\pi-\pi$ stacking interactions were adjusted and rearranged via the temperature-responsive dynamic bonds, thereby improving the thermal stability of the linear aromatic polyurethanes. It indicated that this kind of aromatic polyurethane had a more stable $\pi-\pi$ stacking interaction as the temperature increased. Wang's group[12] developed a light-regulated slide-ring polymer network (PMA-SR), which combined light-responsive azobenzene switches and slide-ring structures. This system can modulate the mechanical properties of the polymer via UV light-induced photoisomerization. UV light induces the azobenzene units to undergo cis−trans photoisomerization, and the formation of the *cis*-configuration restricts the sliding of the macrocycles due to steric hindrance, significantly increasing Young's modulus (by about 93%). However, the elongation and toughness decrease, with the maximum tensile strain decreasing by about 24% and the toughness reduced by 31%. These works declared that the $\pi-\pi$ stacking interaction can be tuned via a matched dynamic chemistry, achieving the control of the material's properties.

In the mechanism of $\pi-\pi$ conjugation, the interaction between the chains can be enhanced with $\pi-\pi$ conjugation. Hence, the interaction of the chains can be tuned by controlling the $\pi-\pi$ conjugation. In this work, photoisomerization of the C═N bond was introduced into the system to control and tune the $\pi-\pi$ conjugation, achieving mechanical performance optimization. The aromatic rings were connected to the polymer chains via the C═N bond. Since C═N bonds have two different stereoisomers (*cis*-isomer and *trans*-isomer) before and after UV light irradiation, the degree of tight packing of the $\pi-\pi$ conjugation structures can be changed. Therefore, this kind of polyurethane elastomer exhibits UV light-controllable mechanical properties. As another characteristic of the conjugated structure, the fluorescence emission effect also exhibits the character of being controllable by UV light. When this material is exposed to UV light, due to the photoisomerization of imine bonds, the distance and stacking structure of the conjugated aromatic rings change, and thus, the fluorescence emission of the conjugated structure also changes. By integrating conjugated aromatic ring structures and photoisomerizable imine bonds onto the polyurethane chains through cooperative integration and regulating the conjugation through photoisomerization, the performance of the linear polyurethane was enhanced, and the fluorescence property was tuned. This provides a new idea for the development of linear and uncross-linked polyurethane materials with high properties and controllable luminescence.

EXPERIMENTAL SECTION

Materials. Benzaldehyde, 1-naphthaldehyde, 2-naphthaldehyde, 2-amino-1,3-propanediol, Polytetramethylene ether glycol (PTMG, M_n = 1000 g· mol^{-1}), dicyclohexylmethane diisocyanate (HMDI), and anhydrous *N*,*N*-dimethylformamide (DMF) were all purchased from Macklin Biochemical. All of the starting reagents and solvents used in the synthesis processes were employed directly without further purification.

Characterizations. *Fourier Transform Infrared Spectroscopy.* Fourier transform infrared (FTIR) spectroscopy measurements were carried out on a Spectrum 100 Fourier transformation infrared absorption spectrometer (Nicolet iS50) from 4000 to 650 cm^{-1} at a resolution of 4 cm^{-1}.

X-ray Diffraction. The crystal fraction of the polymer was detected using a Bruker D8 Advance diffractometer operating in transmission geometry.

Tensile Characterization. The tensile tests of the samples were performed on an instrument (CMT1503, SUST, China) at room temperature with a humidity of approximately 30% and the crosshead speed of 100 mm/min. The width of the dumbbell specimens was 2 mm, and the length was 20 mm. The thickness of the samples was approximately 0.5 mm. Tensile tests were performed on five specimens.

Dynamic Mechanical Analysis. DMA analyses were performed using a NETZSCH DMA242E system. Observations: Strain, 0.1%; frequency, 10 Hz; ramp rate, 3 °C/min; test temperature range, −80 to 80 °C.

UV−vis Absorption Spectroscopy Measurements were performed using a PE Lambda950 UV−vis−NIR spectrophotometer under ambient conditions, with absorbance recorded across the 200−350 nm wavelength range.

Fluorescence Spectroscopy. Measurements were conducted using an Edinburgh FLS980 steady-state and transient fluorescence spectrometer, with fluorescence intensity recorded across the 380−700 nm emission range under 365 nm excitation.

Rheological Characterization. The viscoelasticity of the samples was measured under isothermal conditions at 20 °C using time sweep mode for a duration of 30 min.

Molecule Synthesis. Benzaldehyde, 1-naphthaldehyde, and 2-naphthaldehyde were separately reacted with 2-amino-1,3-propanediol in ethanol to prepare monomers (ID) containing conjugation structures via imine bonds. The reaction proceeded under nitrogen protection at 60 °C for 12 h under reflux, followed by product purification through reduced-pressure distillation. The obtained molecules were named ID-B (benzaldehyde derivative), ID-1N (1-naphthaldehyde derivative), and ID-2N (2-naphthaldehyde derivative).

Polyurethane Preparation. Polyurethanes (PU) containing imine bonds were synthesized via a one-step method. Polytetramethylene ether glycol (PTMG) served as the soft segment, while dicyclohexylmethane diisocyanate (HMDI) and the synthesized monomers with conjugation structure (ID). The specific formulations were as follows: For the PU-B series, the molar ratios of PTMG to ID-B were 1:1, 2:1, 3:1, and 4:1, respectively, with the amount of HMDI equaling the sum of PTMG and ID-B molar ratios to maintain NCO/OH = 1:1. The corresponding products were named PU-B, PU-B2, PU-B3, and PU-B4. PTMG was reacted with ID-1N and ID-2N at a 1:1:2 molar ratio (PTMG/ID/HMDI), with products named PU-1N and PU-2N, respectively. For the control group, propylene glycol (PG) replaced the monomers with a conjugation structure (ID) and was reacted with PTMG and HMDI in a 1:1:2 molar ratio to synthesize the reference sample PU−PG, which contained neither imine bonds nor aromatic side chains. All reactions were conducted under nitrogen protection using anhydrous *N*,*N*-dimethylformamide (DMF) as the solvent at 80 °C for 3 h. The reaction products were subjected to reduced-pressure distillation to remove the solvent, followed by vacuum drying at 80 °C for 24 h to obtain the final polyurethane samples. Fourier transform infrared (FTIR) spectroscopy was employed to detect the urethane bonds (approximately 1700 cm^{-1}, C═O stretching vibration) and imine bonds (approximately 1640 cm^{-1}, C═N stretching vibration). Proton nuclear magnetic resonance (^{1}H NMR) was used to confirm the chemical structures of both the monomers with the conjugation structure (ID) and polyurethanes.

RESULTS AND DISCUSSION

To realize the strategy of enhancing and controlling the properties of PU elastomers, we designed a series of PU elastomers with different contents or different kinds of aromatic ring structures on the PU chains. As shown in

https://doi.org/10.1021/acs.macromol.5c01778
Macromolecules 2025, 58, 9799−9808

Scheme 1. Schematic Diagram of Light-Controlled $\pi-\pi$ Conjugation for Regulating the Properties of Polyurethane

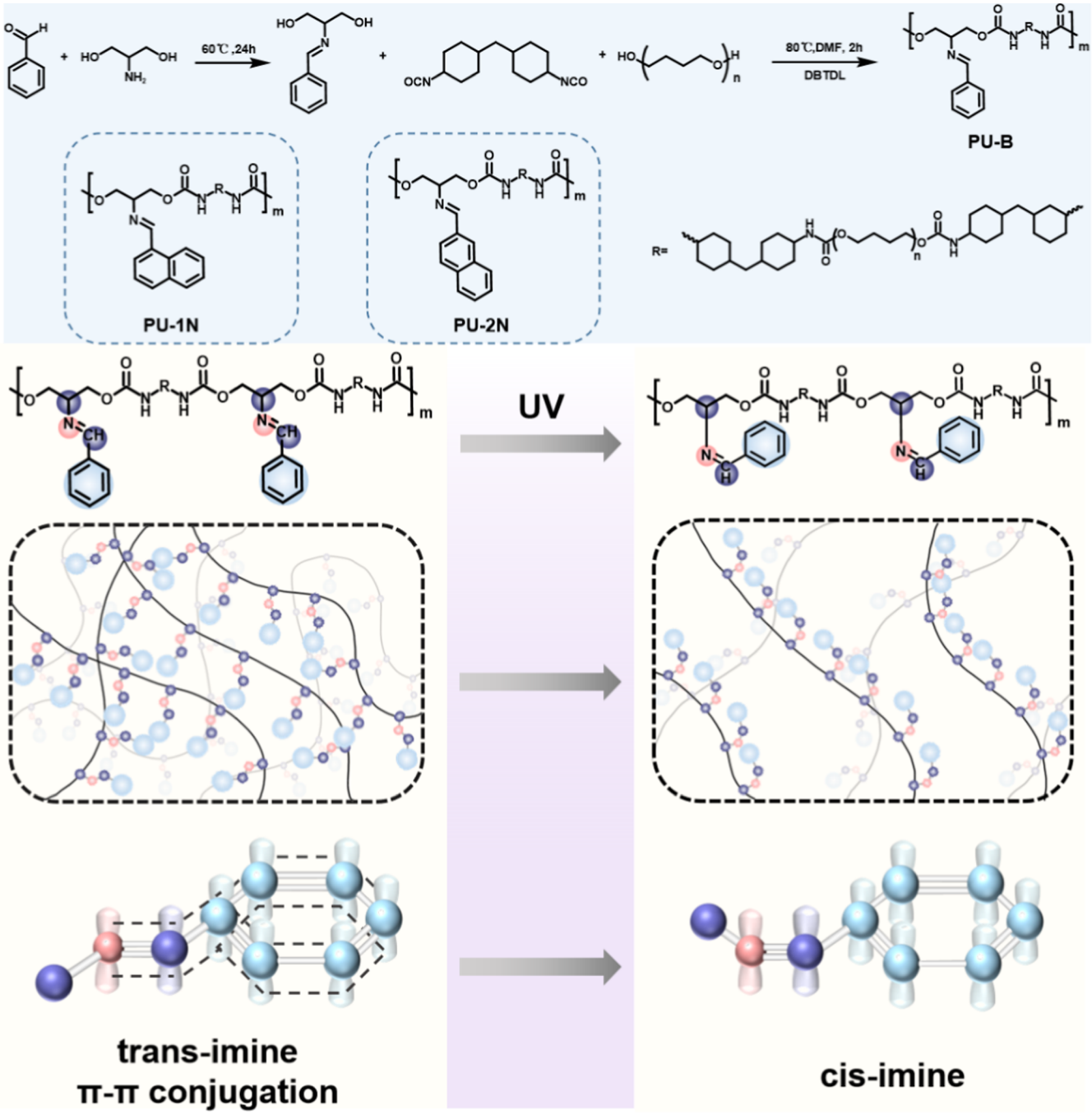

Scheme 1, taking the benzene ring as an example, the conjugated structure was first included into the chain extender molecules, and the photoisomerizable imine bonds were used here to connect the benzene rings to the PU chains. Hence, the arrangement and regularity of the aromatic rings can be controlled by the photoisomerization of the imine bonds. To highlight and prove the preconception and strategy, here, we designed a series of PU with different contents of benzene rings and another series of PU with naphthalene rings on the chains and fixed contents.

Structure Characterization of Polyurethane Elastomers. First, as important properties, the mechanical properties of the PU elastomers were tested. The curves are shown in Figure 1A,B, and the data are summarized in Table S3. Via adjusting the ratio of soft to hard segments (conjugated structure) in polyurethanes, the mechanical properties can be effectively modulated.[13−15] Figure 1A presents the stress−strain curves of the PU-B series polyurethanes. The results demonstrate a clear correlation between the conjugated structure content and mechanical performance. As the molar ratio of conjugated structures to polyurethane soft segments (PTMG) increased systematically from 4:1 (PU-B4) to 1:1 (PU-B), we observed a corresponding progressive enhancement in breaking strength. Specifically, the sample PU-B4 displayed the lowest breaking strength of 6 ± 1.0 MPa. When the content of the monomer with a conjugated structure was increased to produce PU-B3, the breaking strength was improved significantly to 20 ± 1.8 MPa. When further

https://doi.org/10.1021/acs.macromol.5c01778
Macromolecules 2025, 58, 9799−9808

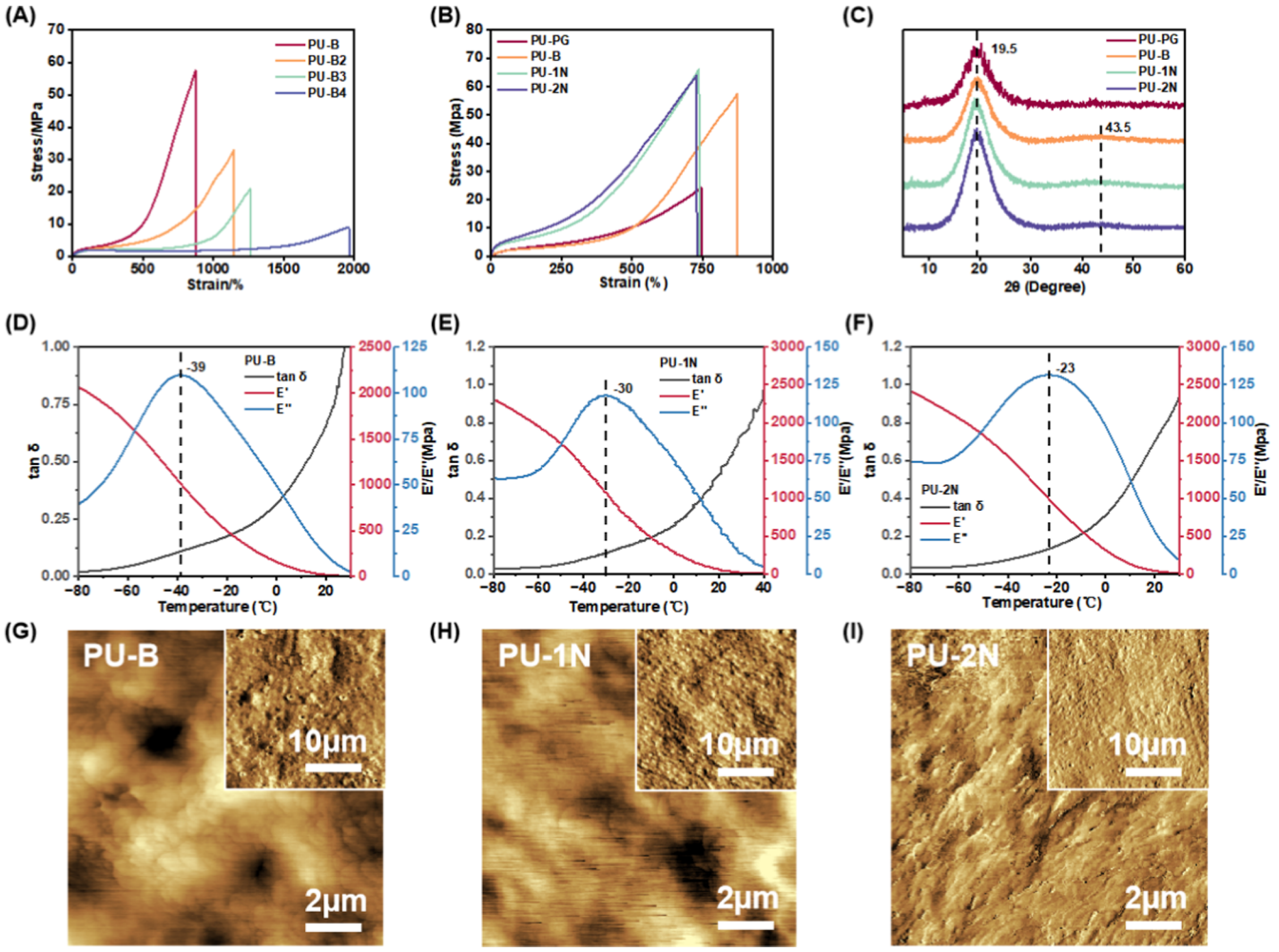

Figure 1. (A) Stress−strain curves of polyurethane with different molar ratios of PTMG and conjugated structures. (B) Stress−strain curves of polyurethanes with different conjugated structures. (C) XRD curves of polyurethane with varying chain structures. (D) DMA curves of PU-B. (E) DMA curves of PU-1N. (F) DMA curves of PU-2N. (G) AFM phase images of PU-B. (H) AFM phase images of PU-1N. (I) AFM phase images of PU-2N.

increased, PU-B2 resulted in a breaking strength of 33 ± 0.6 MPa. Most remarkably, PU-B with the 1:1 ratio of conjugated structures to polyurethane soft segments displayed the breaking strength of 57 ± 0.3 MPa, representing a nearly 10-fold enhancement over PU-B4. In contrast, the elongation at break displayed an inverse correlation with the content of the conjugated structure. The PU-B4 sample, which contained the lowest number of conjugated structures, exhibited the highest elongation at break value of 1847 ± 85%. In comparison, the PU-B3 sample demonstrated reduced ductility with an elongation at break of 1240 ± 57%. This decreasing trend continued with the PU-B2 sample, which showed further reduction to 1065 ± 156%. The PU-B sample, containing the highest conjugated structure content, displayed the lowest elongation at break value of 845 ± 41%. The fracture toughness of the materials also demonstrated significant enhancement (Figure S9), and the PU-B4 sample exhibited a fracture toughness of 52 MJ/m^3. The fracture toughness of the PU-B3 sample increased to 59 MJ/m^3. Further optimization resulted in PU-B2 which demonstrated a substantially enhanced fracture toughness of 112 MJ/m^3. The PU-B sample ultimately achieved the highest fracture toughness value of 128 MJ/m^3 among all of the tested materials. This performance change trend can be primarily attributed to the following factors: First, with the increase in the content of monomers containing conjugated structures with benzene rings (ID-B), the conjugation effect was significantly enhanced between the polymer chains, which led to a higher density of physical cross-linking and an increased number of aromatic rings participating in $\pi-\pi$ stacking interaction per unit volume, ultimately resulting in a substantial improvement in the material's rigidity.[16,17] Second, the decreased soft segment content (PTMG) markedly altered the material's deformation properties, and the expanded conjugated system significantly restricted segmental slippage while substantially increasing energy dissipation during the chain orientation, consequently suppressing macroscopic deformability.[18]

Different kinds of conjugated structures (aromatic rings) were used to observe the effect of $\pi-\pi$ conjugation on the properties, and here, naphthalene rings were used (Figure 1B). It was found that the samples with different aromatic rings incorporated into their side chains (PU-B, PU-1N, and PU-2N) exhibited significantly enhanced breaking strength compared with the control sample PU−PG. Specifically, PU-B achieved a breaking strength of approximately 57 MPa, while PU-1N and PU-2N showed an even higher value of around 63

https://doi.org/10.1021/acs.macromol.5c01778
Macromolecules 2025, 58, 9799−9808

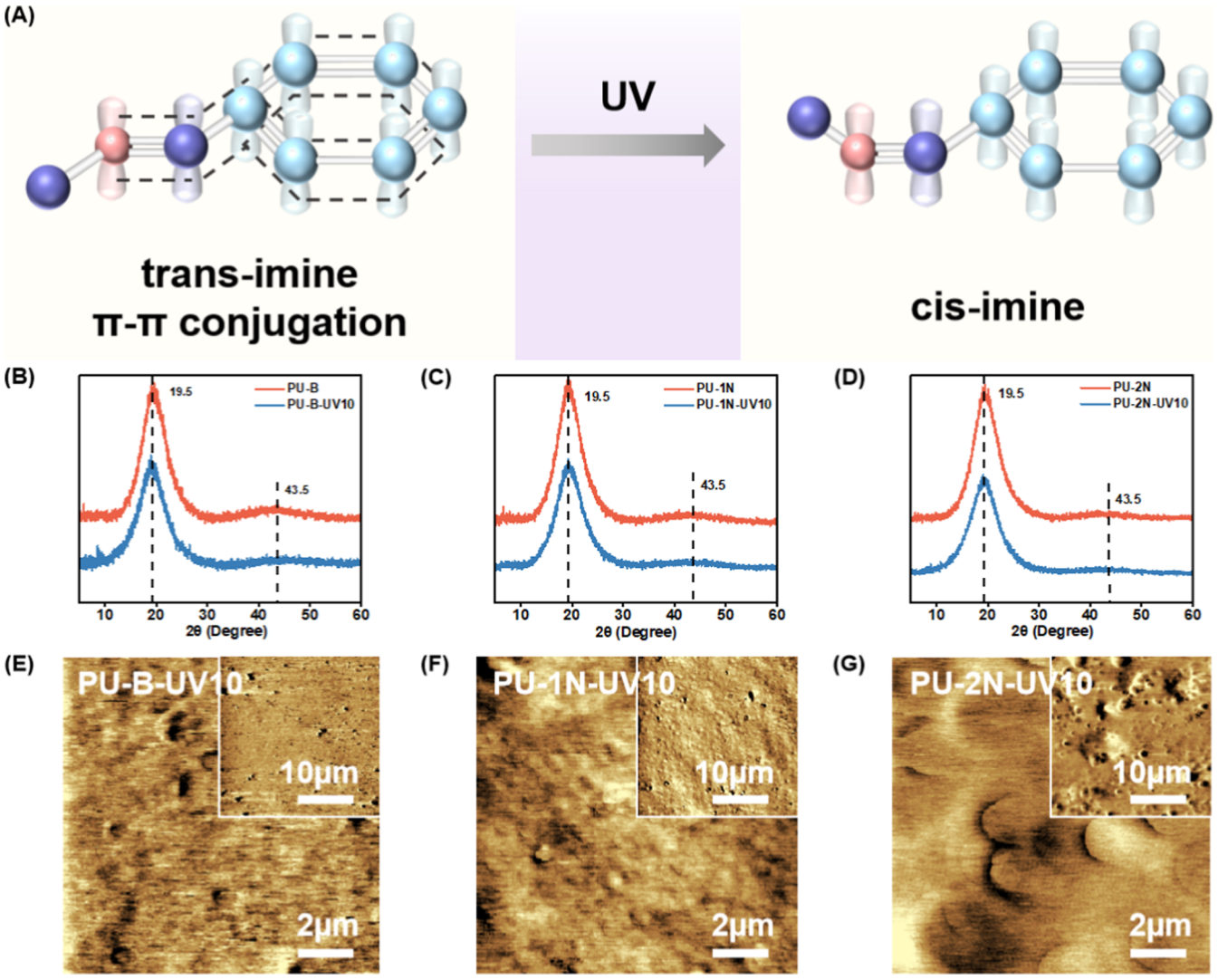

Figure 2. (A) Regulation of cis−trans isomerism of imine bonds by UV light. (B) XRD curves of PU-B and PU-B−UV10. (C) XRD curves of PU-1N and PU-1N−UV10. (D) XRD curves of PU-2N and PU-2N−UV10. (E) AFM phase images of PU-B−UV10. (F) AFM phase images of PU-1N−UV10. (G) AFM phase images of PU-2N−UV10.

MPa. This strengthening effect primarily stems from three factors: First, the rigid structure of the aromatic rings effectively enhances intermolecular interactions between polymer chains. Second, the conjugation effect between imine bonds and aromatic rings further increases the overall rigidity of the material. Additionally, the side-chain aromatic rings may form additional physical cross-linking points via $\pi-\pi$ stacking interaction.[16,19,20] Notably, in terms of elongation at break, PU-B (with benzene rings) exhibited a significant improvement (~844%), while PU-1N and PU-2N (with naphthalene rings) showed little difference from the control sample. This phenomenon can be explained from a molecular perspective: On one hand, the dynamic reversible nature of imine bonds (formation and dissociation) facilitates energy dissipation under external stress. On the other hand, naphthalene rings possess a larger conjugated system and stronger $\pi-\pi$ stacking capability compared with benzene rings. While this interaction enhances strength, it also leads to excessive rigidity in the hard-segment domains, restricting chain mobility and thus preventing significant improvement in elongation at break.[21] This observation was further supported by dynamic mechanical analysis (DMA) (Figure 1D−F). With the increasing conjugation structure of the aromatic rings (benzene ring → 1-naphthalene ring → 2-naphthalene ring), the glass-transition temperature (T_g) of the materials rose from −39 °C to −23 °C, indicating the material's enhanced rigidity. This trend showed complete consistency with the observed results in tensile tests, where an increased modulus coincided with reduced ductility.

To give an insight into the inner structure, the polyurethanes were characterized by X-ray diffraction (XRD) analysis. All four kinds of polyurethane samples exhibited a pronounced broad diffraction peak at $2\theta \approx 20°$, while three of them (PU-B, PU-1N, and PU-2N) additionally showed a weaker broad diffraction peak at $2\theta \approx 44°$ (Figure 1C) except PU−PG. The intense broad peak at 20° primarily originates from the crystallization of the soft segment PTMG, indicating that all samples predominantly exhibit a soft segment-dominated amorphous structure.[22] The existence of $\pi-\pi$ conjugation structure did not significantly influence the overall amorphous characteristics of the soft segment PTMG. The weak broad peak near 44° can be attributed to the $\pi-\pi$ conjugation structure between imine bonds and aromatic rings, which promotes the locally ordered stacking of aromatic rings.[23,24] In

https://doi.org/10.1021/acs.macromol.5c01778
Macromolecules 2025, 58, 9799−9808

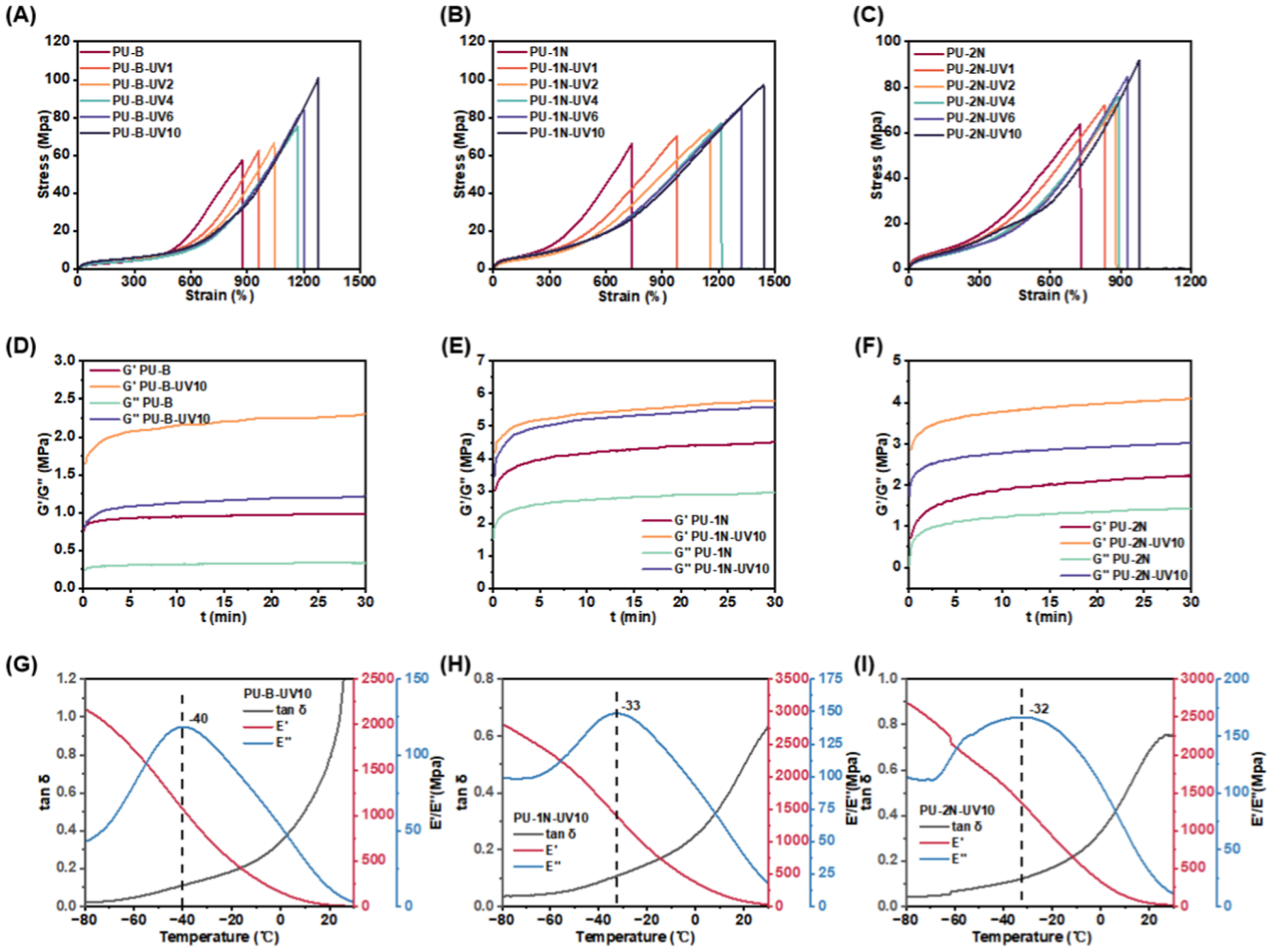

Figure 3. (A) Stress−strain curves of PU-B irradiated by UV light for different times. (B) Stress−strain curves of PU-1N irradiated by UV light for different times. (C) Stress−strain curves of PU-2N irradiated by UV light for different times. (D) Storage modulus (G') and loss modulus (G'') curves of PU-B and PU-B−UV10. (E) Storage modulus (G') and loss modulus (G'') curves of PU-1N and PU-1N−UV10. (F) Storage modulus (G') and loss modulus (G'') curves of PU-2N and PU-2N−UV10. (G) DMA curves of PU-B−UV10. (H) DMA curves of PU-1N−UV10. (I) DMA curves of PU-2N−UV10.

contrast, the control sample PU−PG, which lacks both imine bonds and aromatic ring structures, did not display the corresponding diffraction peak in its XRD curve.

The inner structures of PU-B, PU-1N, and PU-2N samples were also systematically characterized via the atomic force microscopy (AFM) phase imaging mode (Figure 1G−I). Due to the thermodynamic incompatibility between the soft and hard segments in polyurethane elastomers, microphase separation readily occurs. The soft segments, which typically exhibit relatively lower modulus, appear as darker regions in the phase images, while the hard segments with higher modulus are displayed as brighter areas.[25,26] A comparative analysis reveals that all three polyurethane samples demonstrate significant microphase separation characteristics, indicating poor compatibility between their soft and hard segments. Among them, PU-2N exhibits the most distinct phase-separated morphology, with hard segment domains showing clearer and more distributed bright regions. This phenomenon can be attributed to the higher linear symmetry of the 2-naphthalene ring. The two benzene rings of 2-naphthalene extend in a nearly straight-line configuration, which effectively reduces steric hindrance and facilitates closer packing between adjacent naphthalene rings. This distinctive structural characteristic enables the 2-naphthalene planes to maintain parallel orientation more readily, significantly enhancing π-electron cloud overlap and resulting in a more stable stacking. The planarity and linear symmetry of the 2-naphthalene ring promote the formation of a face-to-face $\pi-\pi$ stacking interaction. Such a well-ordered alignment not only increases the binding energy between hard segments but also drives microphase separation, ultimately forming hard segment microdomains with a uniform size distribution. These structural features manifest as evenly distributed bright regions in the atomic force microscopy (AFM) images.

Phototunable Mechanical Properties. Because the conjugated structures are connected to the chains via the imine bonds, the arrangement and regularity of the aromatic rings relative to the main chains are influenced by the conformation of the imine bonds. UV light irradiation alters the cis−trans configuration of imine bonds and the conjugated structures in polyurethanes (Figure 2A).[27,28] Without UV light irradiation, the imine bonds exist in *trans*-configuration, maintaining coplanar alignment with the aromatic rings (benzene/naphthalene rings) to form a highly delocalized

https://doi.org/10.1021/acs.macromol.5c01778
Macromolecules 2025, 58, 9799−9808

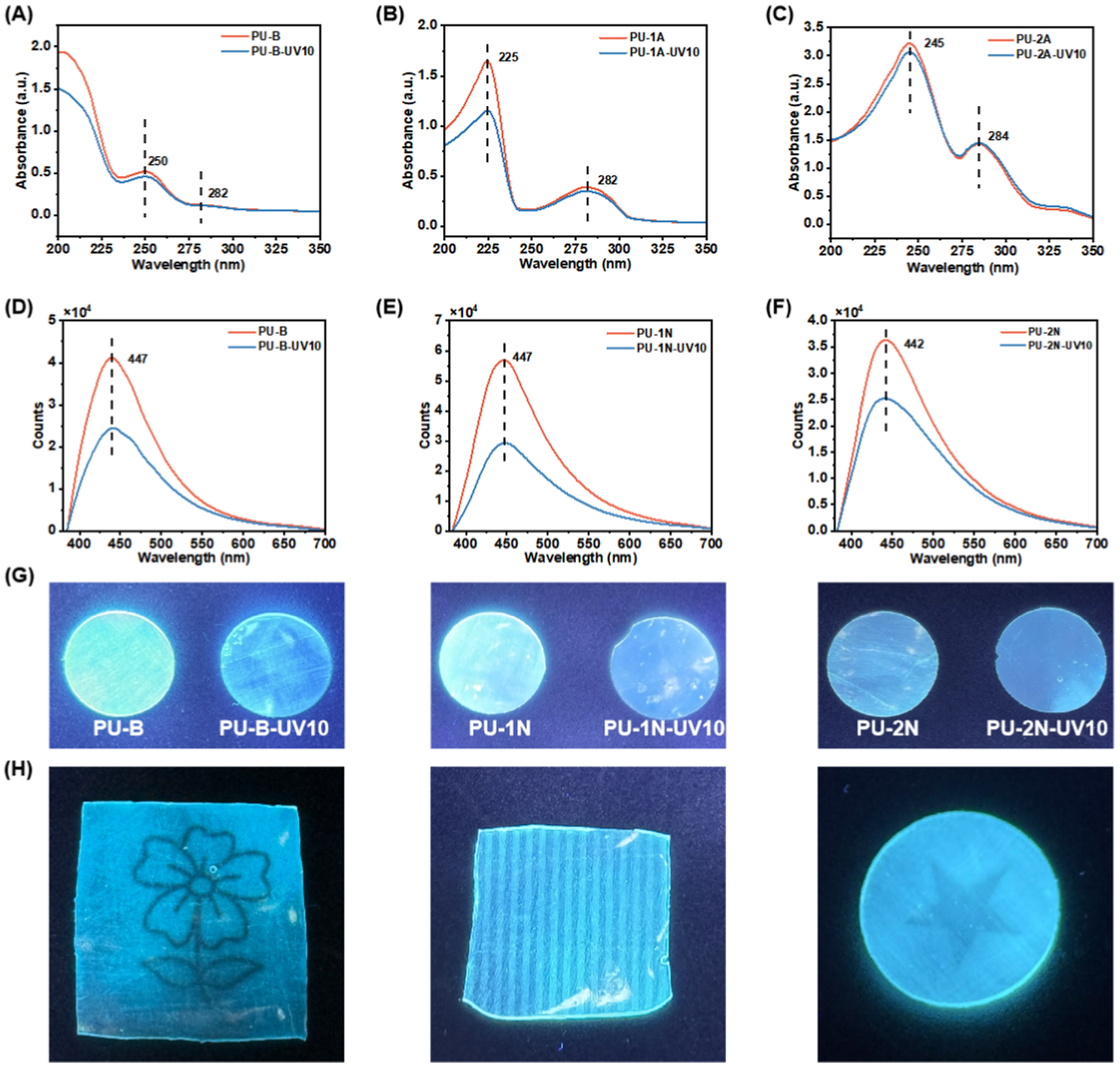

Figure 4. (A) UV−vis absorption spectra of PU-B before and after UV light irradiation for 10 min. (B) UV−vis absorption spectra of PU-1N before and after UV light irradiation for 10 min. (C) UV−vis absorption spectra of PU-2N before and after UV light irradiation for 10 min. (D) Fluorescence spectra of PU-B before and after UV light irradiation for 10 min. (E) Fluorescence spectra of PU-1N before and after UV light irradiation for 10 min. (F) Fluorescence spectra of PU-2N before and after UV light irradiation for 10 min. (G) Photos of different polyurethanes upon UV light irradiation. (H) Photographs of fluorescence patterns and information printed on polyurethane films.

$\pi-\pi$ conjugated system, while the aromatic rings exhibit a typical parallel stacking arrangement. Upon UV light irradiation, imine bonds undergo *cis*-isomerization, disrupting molecular planarity and causing the loss of coplanarity between the aromatic rings and C═N bonds.[29] This leads to conjugated system interruption and hindered electron delocalization, accompanied by a transition from parallel to oblique stacking of aromatic rings. This structure transformation manifests as reduced diffraction peak intensity at $2\theta \approx 44°$ in the XRD patterns (Figure 2B−D). The photoinduced structure rearrangement not only modifies the electronic structure characteristics of the material but also significantly impacts its mechanical properties. Figure 2E−G present the phase images of PU-B, PU-1N, and PU-2N after 10 min of UV light irradiation, showing markedly reduced bright regions (hard segments) compared to the pre-irradiation states. At the 2 μm scale, the boundaries between hard and soft segments become blurred, indicating that UV light-induced *cis*-isomerization of imine bonds disrupts the ordered packing of hard segments.

The changes in the mechanical properties directly demonstrate the regulation of the conjugated structure by UV light and its impact on performance. With prolonged UV light irradiation (from 1 to 10 min), all three series of polyurethane materials (PU-B, PU-1N, and PU-2N) exhibited significant photoresponsive behavior (Figure 3A−C). Among

https://doi.org/10.1021/acs.macromol.5c01778
Macromolecules 2025, 58, 9799−9808

them, the PU-B material demonstrated the most outstanding performance change. The elongation at break increased from 1020% (1 min), 1033% (2 min), 1076% (4 min), and 1089% (6 min) to 1197% (10 min), maintaining excellent ductility. Meanwhile, the breaking strength showed a continuous increasing trend with a prolonged UV light irradiation time, rising from the initial 58 MPa (1 min), 61 MPa (2 min), 73 MPa (4 min), and 85 MPa (6 min) to 99 MPa (10 min). The same photoresponsive characteristics were also verified in the other two systems. The breaking strength of PU-1N increased from 60 to 97 MPa, while its elongation at break significantly rose from 754 to 1430% upon 10 min UV light irradiation. For the sample of PU-2N, breaking strength grew from 64 to 91 MPa, with its elongation at break increasing from 751 to 968%. The change of the mechanical properties can be explained by the change of $\pi-\pi$ conjugation via the *trans*-to-*cis* isomerization of C═N, as discussed previously.[30,31]

The conversion rate from trans-isomerization to *cis*-isomerization showed a monotonically increasing trend with the UV light irradiation time, accompanied by a synchronous enhancement in both fracture strength and elongation at break for flexibility. In the unirradiated state, the *trans*-configured imine bonds formed highly planarized rigid conjugated structures with adjacent aromatic rings. This configuration resulted in tightly packed but mobility-restricted polymer chains, endowing the materials with high rigidity but low toughness. The UV light-induced *cis*-isomerization disrupted the original planarity and introduced steric effects, leading to expanded interchain spacing and significantly enhanced chain segment mobility.[32,33] The conformation changes reduced intermolecular friction resistance, macroscopically manifested as improved elongation at break. Simultaneously, the *cis*-configured imine bonds formed N−H···O hydrogen-bond networks with other oxygen atoms in the soft segments while disrupting the ordered arrangement of aromatic rings. It promoted more uniform dispersion of hard segment microdomains within the soft matrix, resulting in a more homogeneous stress distribution and consequently enhanced fracture strength.[34−36]

The effect of UV light irradiation on the viscoelasticity of polyurethane was investigated with rheometer testing (Figure 3D−F). The test results demonstrated that all samples exhibited significant increases in both storage modulus (G') and loss modulus (G'') after UV light irradiation. The enhancement in G' indicates improved resistance to deformation of the elastomer. The synchronous growth in G'' reflects enhanced internal friction and energy dissipation capacity through the inelastic deformation.[37] The overall enhancement in the storage modulus and loss modulus is closely related to dynamic reorganization of the internal microstructure and changes in intermolecular interactions. Storage modulus refers to the ability of viscoelastic materials to store energy under alternating stress, which can be determined by the degree of entanglement between polymer chains. The configuration transition of imine bonds from *trans*-configuration to *cis*-configuration leads to more complex chain conformations, creating additional physical entanglement points that effectively restrict segments' motion, thereby significantly improving the elastic response. Simultaneously, the *cis*-configuration of imine bonds exposes more polar sites (such as N atoms and aromatic ring electron clouds), forming a denser hydrogen-bonding network with the C═O or N−H groups in polyurethane. These hydrogen bonds act as physical cross-linking points that further strengthen the storage modulus of the material. Meanwhile, the loss modulus reflects the material's ability to dissipate energy under dynamic loading conditions. The segment distortion caused by the *cis*-configuration increases friction resistance between polymer chains, enhancing viscous dissipation effects. During dynamic strain, the reversible breakage and reformation behavior of imine bonds and hydrogen bonds continuously dissipates energy, manifesting as a significant increase in loss modulus (G''). Dynamic mechanical analysis (DMA) results revealed that all three polyurethane samples exhibited varying degrees of reduction in glass-transition temperature (T_g) after UV light irradiation (Figure 3G−I). T_g of PU-B decreased from −39 °C to −40 °C, T_g of PU-1N decreased from −30 °C to −33 °C, and T_g of PU-2N decreased from −23 °C to −32 °C upon 10 min UV light irradiation. These results further demonstrate that the photoinduced *cis*-isomerization disrupts the planarity of chains, leading to decreased material rigidity.

Phototunable Fluorescence Character. As another characteristic of the conjugated structure, the fluorescence emission effect can be controlled by UV light, which makes the material able to be used in the area of information storage.[38−43] The UV−vis absorption spectroscopy and fluorescence spectroscopy analyses were used here to prove the UV light-controllable fluorescence emission.[44] In Figure 4A, a notable decrease of characteristic absorbance in the region of 200−300 nm was shown, which is attributable to the *trans*-configuration to *cis*-configuration transition of imine bonds. This transformation distorts the conjugated plane and shortens the effective conjugation length, reducing π-electron delocalization energy and ultimately weakening the light absorption capacity.[45] Similar phenomena have also been observed on the curves of PU-1N and PU-2N (Figure 4B,C).

Upon UV light excitation, the fluorescence spectra of the three kinds of polyurethane (PU-B, PU-1N, and PU-2N) (Figure 4D−F) revealed characteristic emission peaks at 445 ± 5 nm for all samples.[46,47] After 10 min of UV light irradiation, the peak of fluorescence intensity decreased by approximately 40%.[48] This fluorescence quenching effect originates from two mechanisms: First, the photoinduced transformation from *trans*-configuration to *cis*-configuration of imine bonds disrupts the conjugated system, reducing the π-electron delocalization range and consequently decreasing the radiative transition probability. Second, the configuration distortion introduces new nonradiative decay channels. These combined effects ultimately lead to reduced fluorescence quantum yield.[49−51] Figure 4G demonstrates that the polyurethane samples emit blue fluorescence when exposed to 365 nm UV light. Notably, after 10 min of UV light exposure, the polyurethane elastomers exhibit a significantly decreased fluorescence intensity.[48] Leveraging this unique characteristic, we can precisely control both the duration and spatial distribution of UV light irradiation with the aid of photomasks to "write" patterns and information onto polyurethane films (Figure 4H), enabling their application in data storage.[52,53]

CONCLUSIONS

The $\pi-\pi$ conjugated interaction was utilized to enhance the mechanical properties of the high-performance linear polyurethane elastomers via the noncovalent cross-linking. By the combination of the $\pi-\pi$ conjugated interaction and photocontrolled *cis*−*trans* isomerization of imine bonds, the mechanical properties of the elastomers exhibit the UV light-controllable character. Meanwhile, the fluorescence of the

https://doi.org/10.1021/acs.macromol.5c01778
Macromolecules 2025, 58, 9799−9808

materials is determined by the conjugated structures, and the fluorescence of the materials can be controlled by UV light via the cis−trans isomerization of imine bonds. The high-performance elastomers can also be used in the area of information storage, with fluorescence patterns written on the materials.

■ ASSOCIATED CONTENT

Supporting Information

The Supporting Information is available free of charge at https://pubs.acs.org/doi/10.1021/acs.macromol.5c01778.

Detailed information about the samples; ^{1}H NMR spectra of the molecules; FTIR spectra of different samples before and after light irradiation; mechanical properties data; recipes of samples; glass-transition temperature (T_g) of samples (PDF)

■ AUTHOR INFORMATION

Corresponding Authors

Jing Bai − *State Key Laboratory of Fluorine and Nitrogen Chemicals, School of Chemical Engineering and Technology, Xi'an Jiao Tong University, Xi'an, Shaanxi 710049, China;* orcid.org/0000-0002-5331-9811; Email: baijing8895@xjtu.edu.cn

Fei Chen − *State Key Laboratory of Fluorine and Nitrogen Chemicals, School of Chemical Engineering and Technology, Xi'an Jiao Tong University, Xi'an, Shaanxi 710049, China;* orcid.org/0000-0002-5395-230X; Email: feichen@xjtu.edu.cn

Authors

Zixin Li − *State Key Laboratory of Fluorine and Nitrogen Chemicals, School of Chemical Engineering and Technology, Xi'an Jiao Tong University, Xi'an, Shaanxi 710049, China*

Xinyu Li − *State Key Laboratory of Fluorine and Nitrogen Chemicals, School of Chemical Engineering and Technology, Xi'an Jiao Tong University, Xi'an, Shaanxi 710049, China*

Zhiqi Zhang − *State Key Laboratory of Fluorine and Nitrogen Chemicals, School of Chemical Engineering and Technology, Xi'an Jiao Tong University, Xi'an, Shaanxi 710049, China*

Complete contact information is available at: https://pubs.acs.org/10.1021/acs.macromol.5c01778

Notes

The authors declare no competing financial interest.

■ ACKNOWLEDGMENTS

The authors thank the National Natural Science Foundation of China (22178278, 52573140), the Shaanxi Province Key Research and Development Program (2025CY-YBXM-158), and the Shaanxi Province Natural Science Foundation Research Program (2025JC-QYCX-043)for the financial support.

■ REFERENCES

(1) Chen, S.; Bi, X.; Sun, L.; Gao, J.; Huang, P.; Fan, X.; You, Z.; Wang, Y. Poly(sebacoyl diglyceride) Cross-Linked by Dynamic Hydrogen Bonds: A Self-Healing and Functionalizable Thermoplastic Bioelastomer. *ACS Appl. Mater. Interfaces* **2016**, *8* (32), 20591−20599.

(2) Wang, S.; Liu, Z.; Zhang, L.; Guo, Y.; Song, J.; Lou, J.; Guan, Q.; He, C.; You, Z. Strong, detachable, and self-healing dynamic crosslinked hot melt polyurethane adhesive. *Mater. Chem. Front.* **2019**, *3* (9), 1833−1839.

(3) Jiang, C.; Zhang, L.; Yang, Q.; Huang, S.; Shi, H.; Long, Q.; Qian, B.; Liu, Z.; Guan, Q.; Liu, M.; Yang, R.; Zhao, Q.; You, Z.; Ye, X. Self-healing polyurethane-elastomer with mechanical tunability for multiple biomedical applications in vivo. *Nat. Commun.* **2021**, *12* (1), 4395.

(4) Burattini, S.; Greenland, B. W.; Merino, D. H.; Weng, W.; Seppala, J.; Colquhoun, H. M.; Hayes, W.; Mackay, M. E.; Hamley, I. W.; Rowan, S. J. A Healable Supramolecular Polymer Blend Based on Aromatic π-π Stacking and Hydrogen Bonding Interactions. *J. Am. Chem. Soc.* **2010**, *132* (34), 12051−12058.

(5) Kong, W.; Yang, Y.; Ning, J.; Fu, X.; Wang, Y.; Yuan, A.; Huang, L.; Cao, J.; Lei, J. A highly stable covalent adaptable network through π-π conjugated confinement effect. *Polymer* **2022**, *252*, 124923.

(6) Sharber, S. A.; Mullin, W. J.; Thomas, S. W. Bridging the Void: Halogen Bonding and Aromatic Interactions to Program Luminescence and Electronic Properties of π-Conjugated Materials in the Solid State. *Chem. Mater.* **2021**, *33* (17), 6640−6661.

(7) Molčanov, K.; Milašinović, V.; Kojić-Prodić, B. Contribution of Different Crystal Packing Forces in π-Stacking: From Noncovalent to Covalent Multicentric Bonding. *Cryst. Growth Des.* **2019**, *19* (10), 5967−5980.

(8) Zheng, Q.; Zhang, Y.; Lu, X. High-performance waterborne polyurethane driven by cation-π interactions for damage visualization and information anti-counterfeiting. *Chem. Eng. J.* **2025**, *505*, 159798.

(9) Du, W.; Sun, S.; Zhao, Z.; Zhao, B.; Zhang, X. Controllable transformation of UCST and LCST behaviors in polyampholyte hydrogels enabled by an association-disassociation theory-based switch mechanism. *Mater. Horiz.* **2025**, *12* (2), 587−598.

(10) Xue, Y.; Lin, J.; Wan, T.; Luo, Y.; Ma, Z.; Zhou, Y.; Tuten, B. T.; Zhang, M.; Tao, X.; Song, P. Stretchable, Ultratough, and Intrinsically Self-Extinguishing Elastomers with Desirable Recyclability. *Adv. Sci.* **2023**, *10* (9), No. e2207268.

(11) Lai, Y.; Kuang, X.; Yang, W. H.; Wang, Y.; Zhu, P.; Li, J. P.; Dong, X.; Wang, D. J. Dynamic Bonds Mediate π-π Interaction via Phase Locking Effect for Enhanced Heat Resistant Thermoplastic Polyurethane. *Chin. J. Polym. Sci.* **2021**, *39* (2), 154−163.

(12) Wang, X.; Yu, C.; Wang, M.; Zhao, S.; Mao, Q.; Wang, Y. Mechanically Tunable Slide-Ring Polymers via Photo-Regulated Topological Control. *Angew. Chem., Int. Ed. Engl.* **2025**, No. e202511493.

(13) Ristić, I.; Cakić, S.; Vukić, N.; Teofilović, V.; Tanasić, J.; Pilić, B. The Influence of Soft Segment Structure on the Properties of Polyurethanes. *Polymers* **2023**, *15* (18), 3755.

(14) Sánchez-Adsuar, M. S.; Pastor-Blas, M. M.; Martín-Martínez, J. M. Properties of Polyurethane Elastomers with Different Hard/Soft Segment Ratio. *J. Adhes.* **1998**, *67* (1−4), 327−345.

(15) Lempesis, N.; in 't Veld, P. J.; Rutledge, G. C. Atomistic Simulation of a Thermoplastic Polyurethane and Micromechanical Modeling. *Macromolecules* **2017**, *50* (18), 7399−7409.

(16) Zhu, C.; Kalin, A. J.; Fang, L. Covalent and Noncovalent Approaches to Rigid Coplanar π-Conjugated Molecules and Macromolecules. *Acc. Chem. Res.* **2019**, *52* (4), 1089−1100.

(17) Son, S. Y.; Kim, J. H.; Song, E.; Choi, K.; Lee, J.; Cho, K.; Kim, T. S.; Park, T. Exploiting π-π Stacking for Stretchable Semiconducting Polymers. *Macromolecules* **2018**, *51* (7), 2572−2579.

(18) Castagna, A. M.; Fragiadakis, D.; Lee, H.; Choi, T.; Runt, J. The Role of Hard Segment Content on the Molecular Dynamics of Poly(tetramethylene oxide)-Based Polyurethane Copolymers. *Macromolecules* **2011**, *44* (19), 7831−7836.

(19) Zhou, K.; Zhang, Q.; Gong, J.; Shen, H.; Luo, H.; Chen, S.; Zhang, X.; Zhang, N.; Pei, X.; Wang, T.; Yang, Y.; Wang, Q.; Zhang, Y. Dynamic Non-Covalent Bonds Powering Enhanced Temporary Shape Retention Temperature and Mechanical Robustness in Shape Memory Polyurethane. *ACS Appl. Mater. Interfaces* **2024**, *16* (46), 64031−64041.

(20) Wood, B. M.; Forse, A. C.; Persson, K. A. Aromaticity as a Guide to Planarity in Conjugated Molecules and Polymers. *J. Phys. Chem. C* **2020**, *124* (10), 5608−5612.
(21) Zhang, H.; Wu, Y.; Yang, J.; Wang, D.; Yu, P.; Lai, C. T.; Shi, A.; Wang, J.; Cui, S.; Xiang, J.; Zhao, N.; Xu, J. Superstretchable Dynamic Polymer Networks. *Adv. Mater.* **2019**, *31* (44), 1904029.
(22) Kojio, K.; Nakamura, S.; Furukawa, M. Effect of side groups of polymer glycol on microphase-separated structure and mechanical properties of polyurethane elastomers. *J. Polym. Sci., Part B: Polym. Phys.* **2008**, *46* (19), 2054−2063.
(23) Rama, I.; Subashini, A.; Nadhiya, M.; Ragavendran, V.; Kanagathara, N.; Ahamed, A. A. Synthesis spectral characterization, SC-XRD, Hirshfeld, DFT and in silico antidiabetic activity of novel imine (E)-N-(2-nitro benzylidene) naphthalene-1-amine, a newly synthesized imine: A theoretical and experimental evaluation. *J. Mol. Struct.* **2023**, *1292*, 136084.
(24) Jiang, Q.; Zhang, Q.; Wu, X.; Wu, L.; Lin, J. H. Exploring the Interfacial Phase and π-π Stacking in Aligned Carbon Nanotube/Polyimide Nanocomposites. *Nanomaterials* **2020**, *10* (6), 1158.
(25) Castagna, A. M.; Pangon, A.; Choi, T.; Dillon, G. P.; Runt, J. The Role of Soft Segment Molecular Weight on Microphase Separation and Dynamics of Bulk Polymerized Polyureas. *Macromolecules* **2012**, *45* (20), 8438−8444.
(26) Raftopoulos, K. N.; Pandis, C.; Apekis, L.; Pissis, P.; Janowski, B.; Pielichowski, K.; Jaczewska, J. Polyurethane-POSS hybrids: Molecular dynamics studies. *Polymer* **2010**, *51* (3), 709−718.
(27) Gahl, C.; Brete, D.; Leyssner, F.; Koch, M.; McNellis, E. R.; Mielke, J.; Carley, R.; Grill, L.; Reuter, K.; Tegeder, P.; Weinelt, M. Coverage-and Temperature-Controlled Isomerization of an Imine Derivative on Au(111). *J. Am. Chem. Soc.* **2013**, *135* (11), 4273−4281.
(28) Amati, M.; Bonini, C.; D'Auria, M.; Funicello, M.; Lelj, F.; Racioppi, R. Synthesis of Heteroaryl Imines: Theoretical and Experimental Approach to the Determination of the Configuration of CN Double Bond. *J. Org. Chem.* **2006**, *71* (19), 7165−7179.
(29) Veselý, D.; Jančík, J.; Weiter, M.; Blasi, D.; Ivanova, N.; Krajčovič, J.; Georgiev, A. Fast E/Z UV-light response T-type photoswitching of phenylene-thienyl imines. *J. Photochem. Photobiol., A* **2022**, *430*, 113994.
(30) Zhang, Z.; Jiang, X.; Ma, Y.; Lu, X.; Jiang, Z. High-Performance Branched Polymer Elastomer Based on a Topological Network Structure and Dynamic Bonding. *ACS Appl. Mater. Interfaces* **2023**, *15* (36), 43048−43059.
(31) Guo, Z.; Lu, X.; Wang, X.; Li, X.; Li, J.; Sun, J. Engineering of Chain Rigidity and Hydrogen Bond Cross-Linking toward Ultra-Strong, Healable, Recyclable, and Water-Resistant Elastomers. *Adv. Mater.* **2023**, *35* (21), 2300286.
(32) Yue, C.; Deng, J.; Pang, B.; Liu, G.; Wang, Y.; Xu, H.; Qu, S.; Liu, Y.; Liu, Y.; Zhang, Z.; Zhou, H.; Yan, X. Light-Induced Transformation from Covalent to Supramolecular Polymer Networks. *ACS Macro Lett.* **2025**, *14* (2), 169−175.
(33) Qi, X.; Zhang, Y.; Zhang, L.; Yue, D. Bioinspired Sustainable Polymer with Stereochemistry-Controllable Thermomechanical Properties. *Macromolecules* **2023**, *56* (2), 416−425.
(34) Zhang, Y.; Wang, C.; Pei, X.; Wang, Q.; Wang, T. Shape memory polyurethanes containing azo exhibiting photoisomerization function. *J. Mater. Chem.* **2010**, *20* (44), 9976−9981.
(35) Yan, R.; Jin, B.; Luo, Y.; Li, X. Optically healable polyurethanes with tunable mechanical properties. *Polym. Chem.* **2019**, *10* (18), 2247−2255.
(36) Zhao, L.; Sun, Y.; Liu, X.; Hong, L.; Niu, J.; Zhao, C. Synthesis and characterization of mechanical-controllable polyurethane derived from tetramethybiphenyl epoxy acrylate. *Mater. Today Commun.* **2020**, *24*, 101214.
(37) Heijboer, J. Modulus and damping of polymers in relation to their structure. *Br. Polym. J.* **1969**, *1* (1), 3−14.
(38) Le, X.; Lu, W.; He, J.; Serpe, M. J.; Zhang, J.; Chen, T. Ionoprinting controlled information storage of fluorescent hydrogel for hierarchical and multi-dimensional decryption. *Sci. China Mater.* **2019**, *62* (6), 831−839.
(39) Jian, Y.; Le, X.; Zhang, Y.; Lu, W.; Wang, L.; Zheng, J.; Zhang, J.; Huang, Y.; Chen, T. Shape Memory Hydrogels with Simultaneously Switchable Fluorescence Behavior. *Macromol. Rapid Commun.* **2018**, *39* (12), 1800130.
(40) Ma, C.; Lu, W.; Yang, X.; He, J.; Le, X.; Wang, L.; Zhang, J.; Serpe, M. J.; Huang, Y.; Chen, T. Bioinspired Anisotropic Hydrogel Actuators with On-Off Switchable and Color-Tunable Fluorescence Behaviors. *Adv. Funct. Mater.* **2018**, *28* (7), 1704568.
(41) Le, X.; Shang, H.; Wu, S.; Zhang, J.; Liu, M.; Zheng, Y.; Chen, T. Heterogeneous Fluorescent Organohydrogel Enables Dynamic Anti-Counterfeiting. *Adv. Funct. Mater.* **2021**, *31* (52), 2108365.
(42) Liu, H.; Wei, S.; Qiu, H.; Zhan, B.; Liu, Q.; Lu, W.; Zhang, J.; Ngai, T.; Chen, T. Naphthalimide-Based Aggregation-Induced Emissive Polymeric Hydrogels for Fluorescent Pattern Switch and Biomimetic Actuators. *Macromol. Rapid Commun.* **2020**, *41* (13), 2000123.
(43) Botiz, I.; Astilean, S.; Stingelin, N. Altering the emission properties of conjugated polymers. *Polym. Int.* **2016**, *65* (2), 157−163.
(44) Kato, T.; Gon, M.; Tanaka, K. Molecular Design for Luminescent Azobenzene-Containing Conjugated Polymers and Their Application to Film Sensors for Recording Acid Exposure History. *Macromol. Rapid Commun.* **2025**, No. e00371.
(45) Luo, Y.; Utecht, M.; Dokić, J.; Korchak, S.; Vieth, H. M.; Haag, R.; Saalfrank, P. cis-trans Isomerisation of Substituted Aromatic Imines: A Comparative Experimental and Theoretical Study. *ChemPhysChem* **2011**, *12* (12), 2311−2321.
(46) Wang, S. K.; Sung, C. S. P. Fluorescence and IR Characterization of Cure in Polyurea, Polyurethane, and Polyurethane-Urea. *Macromolecules* **2002**, *35* (3), 883−888.
(47) Li, Z.; Pei, S.; Shao, K.; She, X.; Yang, M.; Zhang, K.; Li, H.; Ding, Y.; Hu, X. A Blue Tunable Waterborne Polyurethane-Based Carbon Nitride With Wide Excitation-Wavelength-Dependent Fluorescence. *J. Appl. Polym. Sci.* **2025**, *142* (32), No. e57282.
(48) Huang, G.; Yao, C.; Huang, M.; Zhou, J.; Hao, X.; Ma, X.; He, S.; Liu, H.; Liu, W.; Zhu, C. Colorless Transparent, and High-Performance Polyurethane with Intrinsic Ultraviolet Resistance and Its Anti-UV Mechanism. *ACS Appl. Mater. Interfaces* **2023**, *15* (14), 18300−18310.
(49) Rondão, R.; Seixas de Melo, J.; Melo, M. J.; Parola, A. J. Excited-State Isomerization of Leuco Indigo. *J. Phys. Chem. A* **2012**, *116* (11), 2826−2832.
(50) Golovkova, T. A.; Neckers, D. C.; Kozlov, D. V. Synthesis and Properties of Novel Fluorescent Switches. *J. Org. Chem.* **2005**, *70* (14), 5545−5549.
(51) Escudero, D. Revising Intramolecular Photoinduced Electron Transfer (PET) from First-Principles. *Acc. Chem. Res.* **2016**, *49* (9), 1816−1824.
(52) Hou, H.; Hu, K.; Lin, H.; Forth, J.; Zhang, W.; Russell, T. P.; Yin, J.; Jiang, X. Reversible Surface Patterning by Dynamic Crosslink Gradients: Controlling Buckling in 2D. *Adv. Mater.* **2018**, *30* (36), 1803463.
(53) Shi, J.; Wang, Z.; Zheng, T.; Liu, X.; Guo, B.; Xu, J. Thermal and UV light adaptive polyurethane elastomers for photolithography-transfer printing of flexible circuits. *Mater. Horiz.* **2022**, *9* (12), 3070−3077.

https://doi.org/10.1021/acs.macromol.5c01778
Macromolecules 2025, 58, 9799−9808